Calibrating Surface Weather Observations to Atmospheric Attenuation Measurements

B. Sanii[1]

A correlation between near-infrared atmospheric attenuation measurements made by the Atmospheric Visibility Monitor (AVM) at the Table Mountain Facility and airport surface weather observations at Edwards Air Force Base has been performed. High correlations (over 0.93) exist between the Edwards observed sky cover and the average AVM measured attenuations over the course of the 10 months analyzed. The statistical relationship between the data sets allows the determination of coarse attenuation statistics from the surface observations, suggesting that such statistics may be extrapolated from any surface weather observation site. Furthermore, a superior technique for converting AVM images to attenuation values by way of MODTRAN predictions has been demonstrated.

I. Introduction

A statistical description of optical atmospheric attenuation is one of the goals of the Optical Communications Group at the Jet Propulsion Laboratory, particularly at specific laser spectral bands. Until now, statistics have been determined using the data collected by three Atmospheric Visibility Monitors (AVMs). Recently, reports on the possible use of surface weather observations [1] for sky-cover modeling have prompted using AVM data to calibrate the qualitative surface weather observations to quantitative attenuation statistics. Because the surface weather observation sites are numerous and distributed over most of the United States (they are frequently at airports), the possibility of a statistical description of the atmospheric attenuation over the entire nation exists. This article describes the correlation between a single AVM and a single surface observation station. Further analysis corroborating these results using a second AVM site is currently being performed.

A. The Atmospheric Visibility Monitoring Program

The AVM program consists of three autonomous observatories connected to the Jet Propulsion Laboratory (JPL) by network. Each of the three observatories (Fig. 1) is stationed in the southwestern

---

[1] Communications Systems and Research Section.

This paper will also be published in *Free-Space Laser Communication Technologies XIII*, G. S. Mecherle, Editor, Proceedings of SPIE, vol. 4272, in press, 2001.

The research described in this publication was carried out by the Jet Propulsion Laboratory, California Institute of Technology, under a contract with the National Aeronautics and Space Administration.

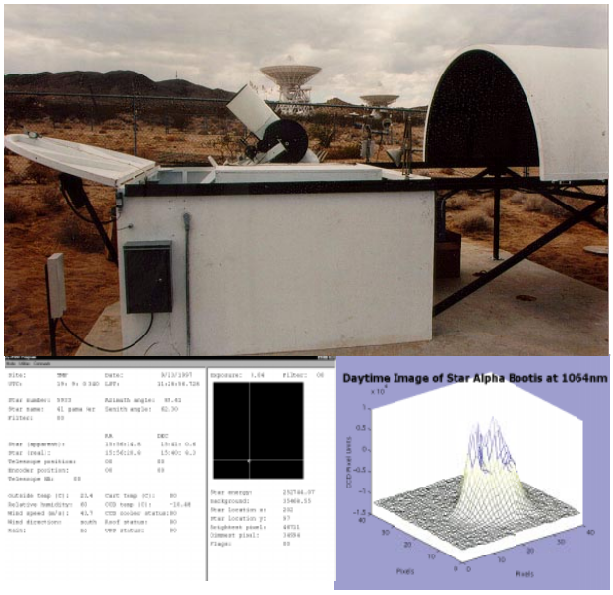

Fig. 1. The Table Mountain AVM (top), a screen shot of the custom program (bottom left), and a sample of an acquired star image (bottom right).

United States; they are located at Mt. Lemmon (near Tucson, Arizona), the Table Mountain Facility (near Wrightwood, California), and the Goldstone Deep Space Communications Complex (near Barstow, California). The three sites have been upgraded [2] and are now gathering data using new processors, software, and cameras with greater near-infrared sensitivity and dynamic range. The sites are also networked to an atomic clock gateway, ensuring that they are on the same schedule and permitting accurate site-diversity statistics to be tabulated.

Using motorized autonomous telescopes, the observatories take photometric readings of a set of bright stars through six optical filters. Three of these filters pass a narrow bandwidth of light (10 nm) that corresponds to laser wavelengths that may be used in future free-space optical communications systems, including 532 nm (a frequency-doubled Nd:YAG laser), 1064 nm (the fundamental Nd:YAG wavelength), and 860 nm (a common diode laser). In addition to these, there are three other broadband astronomical filters in place: the visual, infrared, and blue filters. Each observatory is completely automated, with environmental controls and alarms, and is capable of both day and night observing.

Post-processing enables the determination of a zenith-normalized attenuation value for every measurement. This process is described in greater detail below, where the new calibration technique is discussed. The new calibration technique employs the software tool of MODTRAN, which is an accepted standard for determining the spectral absorption and scattering of the atmosphere [3].

B. Surface Weather Observations

The surface weather observations at Edwards Air Force Base used in this study are from the records gathered by the National Climatic Data Center (NCDC) from sites across the Unites States, and are readily available for purchase at nominal fees. Certified observers, using standards described in the Federal Meteorological Handbook (FMH) [4], record hourly observations. Most of the surface weather observation sites are at airports.

Each observation consists of 23 fields, of which only the station, date, time, visibility, and sky cover are used in this article. Sky cover is defined by the FMH as “the amount of the celestial dome hidden by

clouds and/or obscurations,"[2] and is expressed in four categories that are defined by how many eighths of the sky are obscured.

The four categories used at Edwards are

(1) Clear—No obscurations

(2) Scattered—Any to 4/8 of the sky covered

(3) Broken—5/8 to 7/8 of the sky covered

(4) Overcast—Complete coverage of the celestial dome

It should be noted that the FMH describes a fifth category, "few," which was not implemented at Edwards for the dates of analysis. Edwards is approximately 65 km from Table Mountain and about 1000 m lower in elevation, although line of sight exists between the two.

II. Analysis

A. The AVM Calibration Technique

The AVM measurements can be converted into transmission values by several methods. By comparing measurements taken at different elevation angles (corresponding to different line-of-sight air masses), a value may be extrapolated that corresponds to a measurement at zero air mass (above the atmosphere). Previously, a standard exponential attenuation model of the atmosphere was used, producing a calibration value as shown in Fig. 2. By extrapolating back out to zero air mass, the projected intensity above the

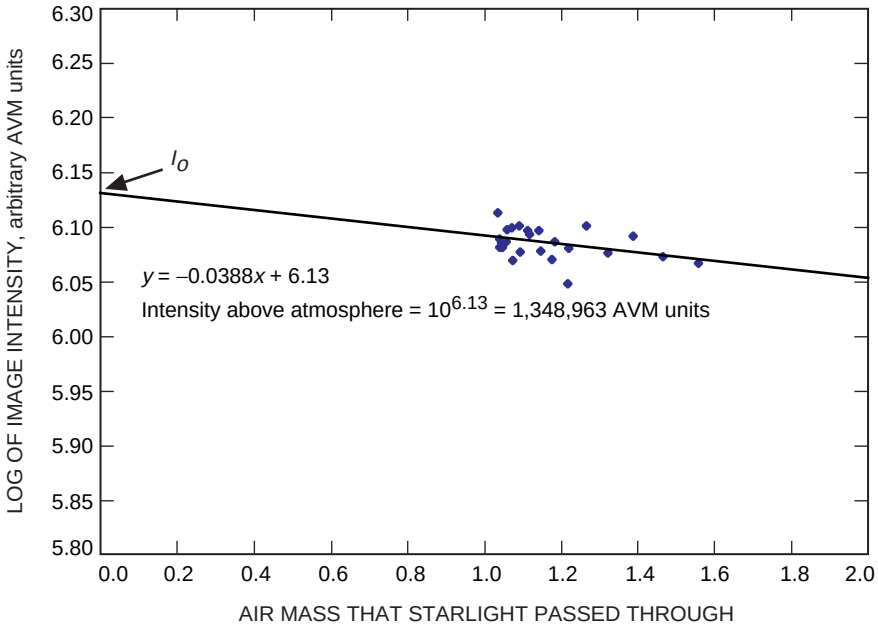

Fig. 2. A calibration plot where the log of intensities of the day's images is plotted against the air mass traversed as the star's apparent position moves across the sky (Table Mountain AVM, May 17, 2000, star 5340, 860 nm).

[2] *Surface Weather Observations and Reports*, Federal Meteorological Handbook (FMH) Number 1, National Weather Service, Section 9.3.a. http://www.nws.noaa.gov/oso/oso1/oso12/fmh1/fmh1ch9.htm#chp9link.

atmosphere is determined. This intensity (labeled I_o) is the value that is used to calibrate AVM data to an attenuation measurement. The slope of the line corresponds to the transmission at zenith (one air mass), and this plot shows a transmission of 91 percent, which is about 10 percent greater than MODTRAN predictions for a clear day, and thus is of low confidence.

The exponential model is producing attenuations that are unphysical, and thus it is proving to be inadequate. Because the points in Fig. 2 are relatively co-linear, it is suspected that the exponential model's shortcomings are toward the lesser air masses, where the AVM has less data. Consequently, while a new model is being developed, MODTRAN predictions are being used to determine the calibration constant.

This is done by solving the following equation for the calibration value I_o:

$$\text{attenuation (db)} = -10 \log \left(\frac{\text{energy}}{\text{exposure} \times I_o} \right)^{1/\text{air mass}} \tag{1}$$

where energy is the measured energy of the star in pixel values, exposure is its shutter-open time in seconds, air mass is the mass of air that the star's light traversed (1 is normalized to zenith), and I_o is the calibration constant that corresponds to the energy/exposure ratio that the AVM would have measured if it were above the atmosphere.

The attenuation is set to the MODTRAN prediction for the altitude and wavelength of the measurement; the air mass is derived from the elevation of the star at the time of the measurement; and the energy represents the measurement itself. By performing this conversion on a set of measurements for one star, through one filter, a significant range of possible calibration values is produced for each day. Selecting the best one is a non-trivial task; on the one hand, one would want to select the greatest measurement in the entire set, because this is likely to be an image taken when the atmospheric condition is photometric and thus most closely matches the MODTRAN prediction. On the other hand, one must account for time degradation of the AVM system's optical transmission due to dust gathering on the exposed optical surfaces. This means that a single calibration value will not suffice and a time-varying calibration value set is necessary. Experience showed that using the greatest calibration value for a rolling 2 week window produced a high likelihood of catching at least one clear-atmosphere image and at the same time tracked the gradual optical degradation of the AVM system. By calibrating to MODTRAN, the calibration constants are more consistent and centered about a more realistic value than by way of the exponential model. Calibration values determined by this method are shown in Fig. 3.

Using this set of calibration values, attenuation was determined for observations throughout the year 2000. Figure 4 presents these values as a cumulative distribution function (CDF). This format is useful for optical communication mission designers, who need to know what percentage of the time they can expect to have a given (or better) transmission through the atmosphere. Further work can be done refining the MODTRAN model for better calibration, perhaps by way of FASCOD3 seasonal atmospheric compensations.

B. Surface Weather Observation Correlation

Because the surface weather data and the AVM data are both time tagged, it is possible to merge the data sets by way of Microsoft Access. Once merged, a statistical correlation of various subsets is possible, yielding a relationship between the two. This relationship can be used to supplement AVM data for when system outages occur as well as to synthesize results from the larger database that extends to before the AVM program began. Furthermore, this allows the possibility of synthesizing attenuation statistics at other observation sites around the country and correcting for altitude differences by way of MODTRAN predictions.

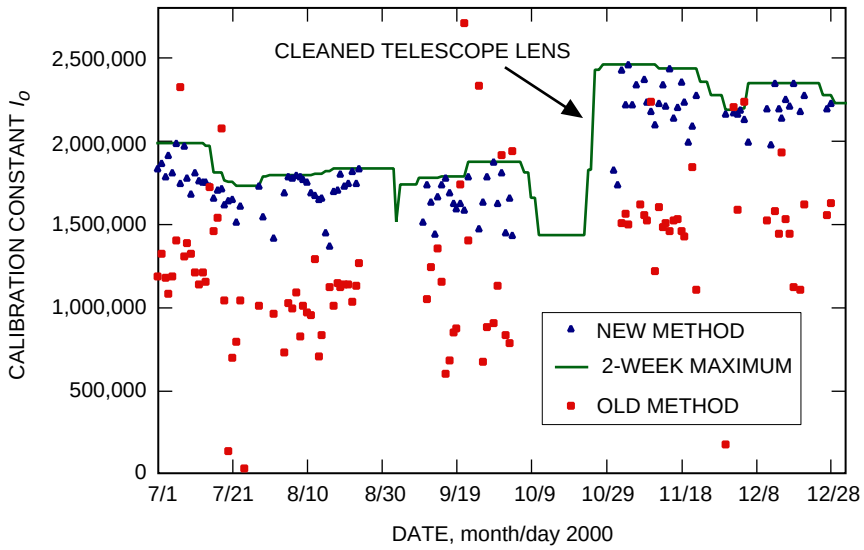

Fig. 3. Daily calibration values using the old method, new method, and 2-week maximum of the new method. On November 1, the telescope's Schmidt corrector was cleaned, and the expected calibration value increase can be observed. (Images of Alpha-Boo through an 860-nm filter.)

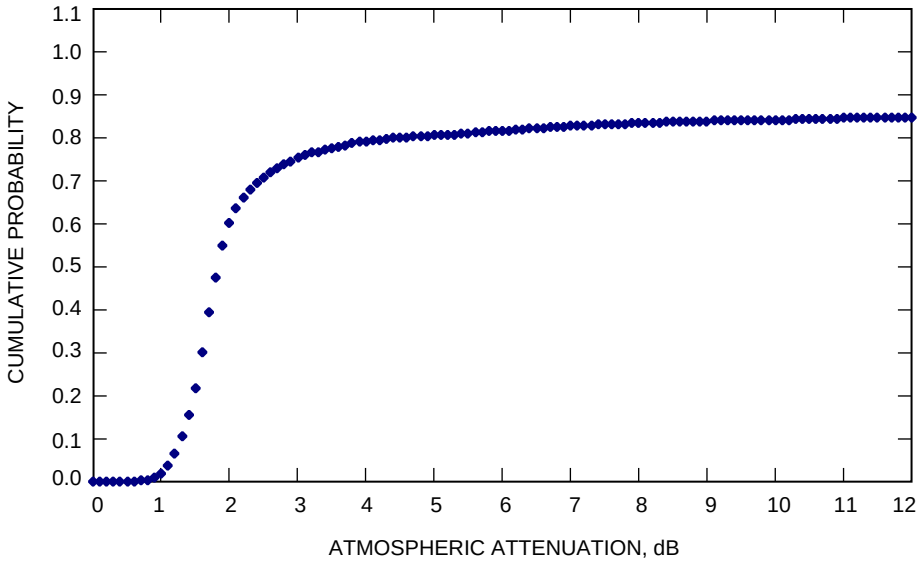

Fig. 4. A CDF for the attenuation observed at Table Mountain through an 860-nm narrowband filter, using the new MODTRAN calibration method (January 1, 2000, to December 28, 2000, star 5340).

The analysis concentrates on the relationship between AVM attenuation measurements and the surface observed cloud cover. Other surface observations, such as visibility and cloud altitude, were also investigated for a useful relationship to attenuation measurements, but with little success. The correlation values between the AVM measured average attenuations, and the observed visibilities and cloud altitudes are 0.62 and 0.46, respectively (with 10 and 15 degrees of freedom, respectively). Good correlations were not expected because AVM measures attenuation along a vertical path, and these observations have ramifications largely in horizontal attenuation.

The process began by binning the AVM measured attenuations into groups based on the surface observed cloud cover at the time of the measurement. For each cloud-cover category, a distribution of measured attenuations was determined; results are presented in Fig. 5. The distributions spread significantly as one experiences more severe cloud cover, and the mean attenuation for each cloud-cover bin increases.

The AVM system has a fundamental threshold: if it cannot see the star, it cannot determine the precise attenuation. Generally this sensitivity threshold is about 10-dB attenuation at 860 nm, but it varies with wavelength, star intensity, and current sky background. When this occurs, the star is considered "blocked" for communication purposes, and the measurement is assigned an arbitrarily high number of 30 dB. To correctly correlate AVM and surface weather data, two sets of statistics are tracked: the average attenuation when the AVM could "see" the star and the percentage of the time when the AVM could not "see" the star. These statistics are binned according to the sky cover observed simultaneously at Edwards and are presented in Fig. 6.

By converting the sky-cover categories to their average percentage of cloud cover (using the definitions presented in the introduction), a correlation between the statistics of Fig. 6 and the cloud cover may be performed. This yields correlation coefficients of 0.930 between the sky cover and the average simultaneously reported attenuation, and 0.998 between the sky cover and the percentage of time blocked. Both values have two degrees of freedom.

One may be concerned that the percentage of time blocked does not end at 100 percent (when it is presumably completely overcast). The explanation seems to lie in the greater sensitivity of the AVM system to that of the human eye; a visibly overcast day may still be somewhat transparent to the AVM. The camera is configured to allow exposures of up to 15 seconds (compared to about 1/10 s in the human eye), and its telescope's aperture is 254 mm (approximately 30 times that of the eye). This is corroborated by the time of day when these "erroneous" observations take place. The majority of these observations occur around twilight, when the human eye's response is worse and while the AVM can still perform its long exposures (because the sky is not very bright yet). The discorrelation is apparently not a function of the distance between Edwards and Table Mountain. The argument for this is built by isolating the erroneous points (unblocked measurements when it was overcast or blocked measurement

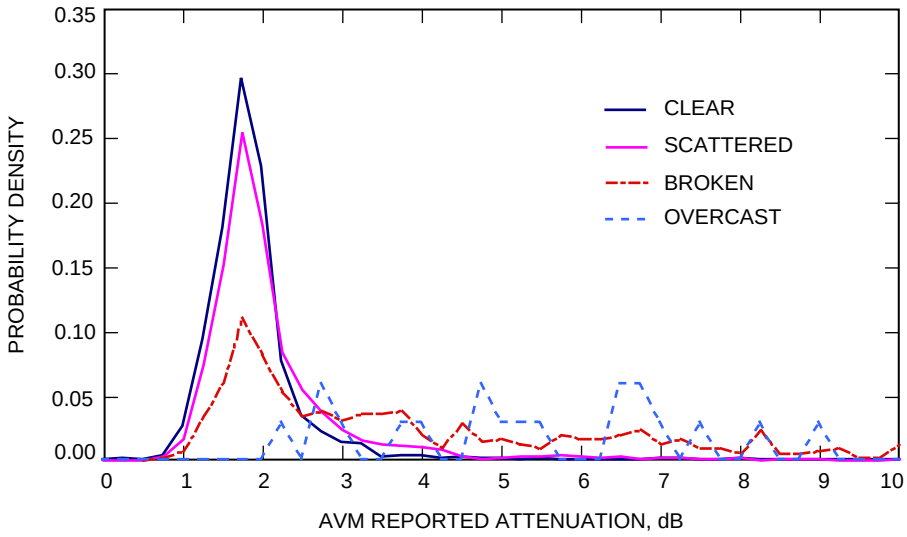

Fig. 5. Distributions of measured attenuations seen at Table Mountain when Edwards reported a given sky-cover category (all of 2000, 860 nm, star 5340).

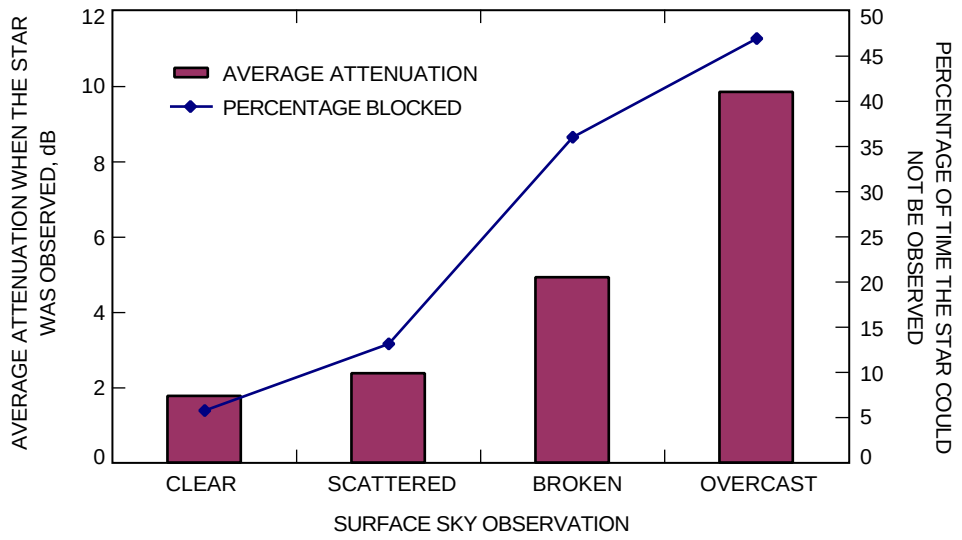

Fig. 6. For each sky category, the corresponding AVM data set was analyzed, showing the average attenuations and the percentage of blocked images (i.e., beyond the sensitivity of the AVM, thus very attenuated).

when it was clear) and plotting the azimuth of the AVM measurement at that time. If distance were the issue, one would expect a cluster of erroneous measurements on the west, opposite the direction to Edwards. In fact, there was no discernable pattern in these points.

C. Determining Surface Observation Attenuation Statistics

With the added confidence of these high correlation values, the next task was to invert the analysis and use the surface weather observations to statistically predict the attenuation. This process consists largely of bookkeeping; one multiplies the number of observations of a particular sky-cover category by the determined "percentage of time blocked" and records that as a 30-db attenuation (the arbitrarily high one). The remaining observations are given an attenuation equal to the average unblocked attenuation of their respective categories. This process is repeated for each surface weather category and can be seen in Table 1, with the cumulative distribution function of attenuation presented in Table 2 (using the time period when the TMF AVM was operational between January 1, 2000, and November 17, 2000). As a further check, this cumulative distribution function (CDF) was compared with the one determined from AVM data, shown in Fig. 7.

This process now enables two possible capabilities:

(1) The capability to use other surface weather observation sites to generate local atmospheric attenuation statistics (correcting for local elevation by way of MODTRAN)

(2) The ability to supplement the data set for the AVM at Table Mountain, correcting for system outages

The first is being pursued by comparing the Goldstone AVM and the nearby Barstow-Daggett airport observations, but to initial appearances more AVM observations from Goldstone will be needed before that study may be performed.

The second can be readily demonstrated by examining the Table Mountain AVM data set and isolating outages. This is a particularly important demonstration, because the system outages for the majority

Table 1. An example of the bookkeeping for determining the attenuation statistics.

Sky category	Number of observations (X)	Percentage of measurements blocked (known percentage B)	Number at 30 dB ($X \times B$)	Average attenuation (known average A)	Number at average attenuation ($[1 - B] \times X \times A$)
Clear	1865	5.791	108.002	1.75658	1756.998
Scattered	2570	13.074	336.002	2.354053	2233.998
Broken	650	36.000	234	4.936654	416
Overcast	64	46.875	30	9.827009	34

Table 2. The general cumulative distribution function.

Attenuation	Number of counts	Probability density	Cumulative distribution
1.75658	1757	0.341231	0.341231
2.354053	2234	0.433871	0.775102
4.936654	416	0.080792	0.855894
9.827009	34	0.006603	0.862498
30	708	0.137502	1

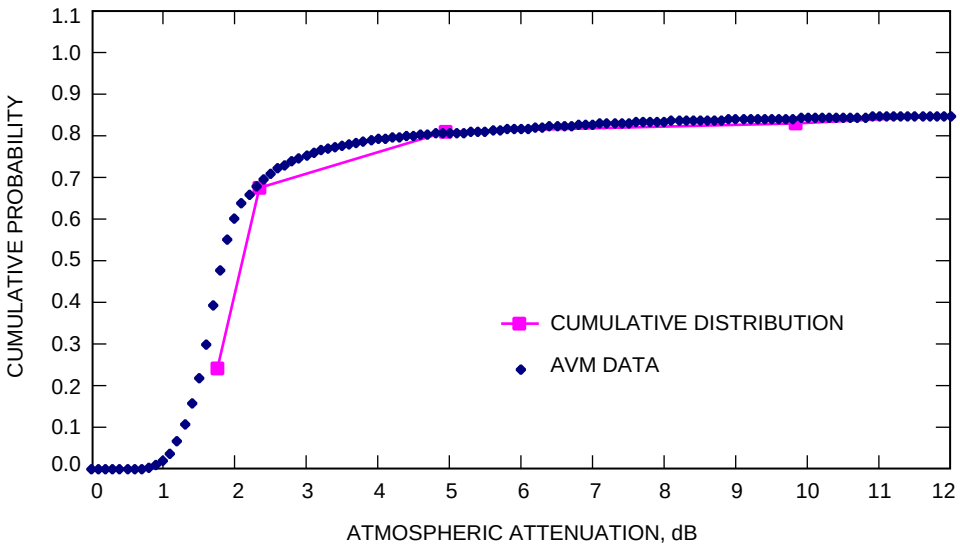

Fig. 7. The CDF of Fig. 4, overlaid with the projected CDF derived from the surface weather observations (January 1, 2000, to December 28, 2000, star 5340, 860 nm, TMF, MODTRAN calibration). While the result is not a surprise, as one set of data was used to calibrate the other, it is a good check for the process.

of the year 2000 were not randomly distributed, but clustered in periods where the probability of cloud cover was greater. The AVM rain-recovery software routines were fixed in November; prior to that, every time it rained the system needed to be manually restarted, often hours to days later (particularly on the weekends). Consequently, valid measurements of rain (which is interpreted as opaque attenuation) and the typically cloudy portion immediately after it stops raining are not included in the set. However, at

Edwards the surface observations continued unhindered. Figure 8 demonstrates the systematic bias of the previous year's AVM data using surface weather observations.

Finally, a cumulative distribution function of the AVM data supplemented by the surface observation data is presented in Fig. 9. This was done by scaling the five CDF points (determined from the surface observation data) by the fraction of the time range they represented. Then the AVM data were similarly scaled, and the two were summed together.

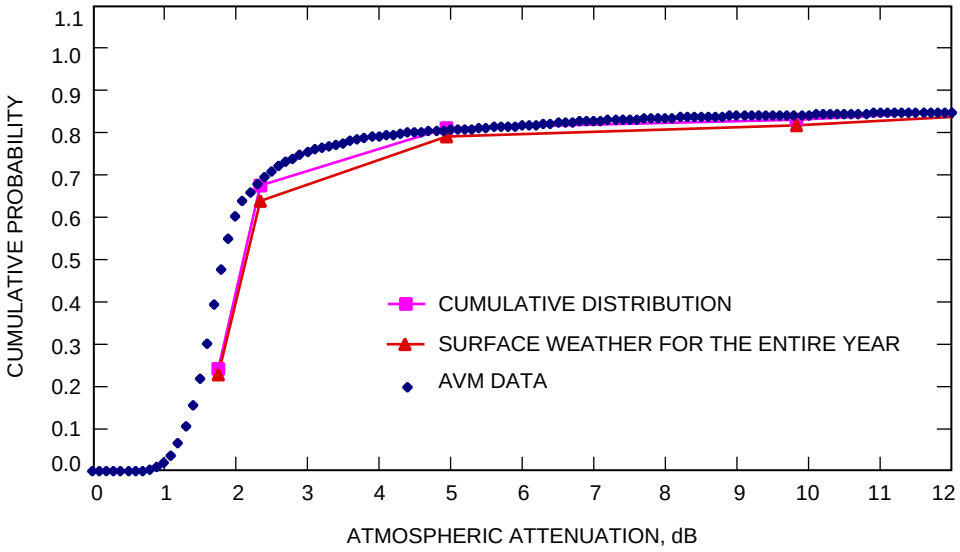

Fig. 8. The projected surface-weather observation CDF derived from the sky-cover ratings of the entire year, as opposed to those of when only the AVM was operational, such as Fig. 7, whose plots are overlaid for reference (January 1, 2000, to December 28, 2000, star 5340, 860 nm, TMF, MODTRAN calibration).

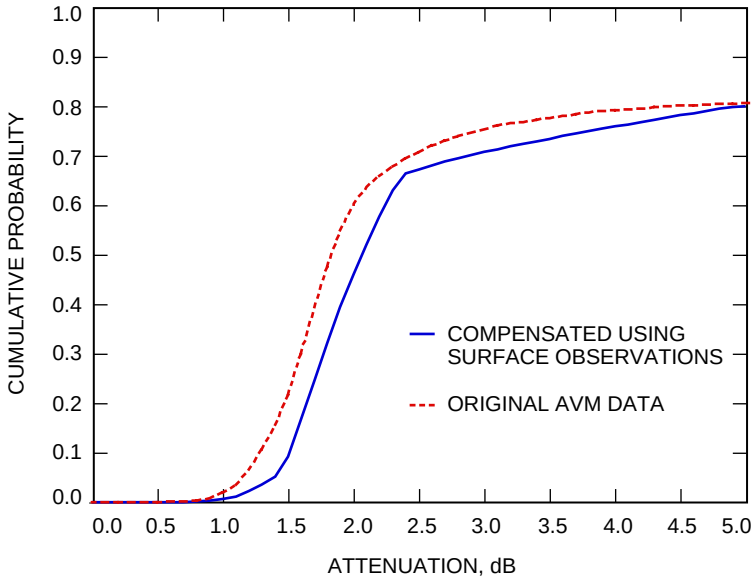

Fig. 9. The combined CDF of the AVM data and the calibrated surface observations for the period when there were no AVM data (January 1, 2000, to November 11, 2000, 860 nm, Table Mountain AVM and Edwards surface observations).

III. Conclusions

A strong correlation exists between the sky-cover surface weather observations performed at Edwards Air Force Base in California and the Atmospheric Visibility Monitor attenuations measured at the nearby Table Mountain between January 1, 2000, and November 11, 2000. The correlation coefficient between the sky-cover observation and the average attenuation measurement is 0.930, and the coefficient between the same and the percentage of time unblocked was 0.998. This high correlation allows attenuation statistics to be determined from the surface observations, to be used in verifying and supplementing the AVM data. Furthermore, a new calibration procedure based on MODTRAN predictions has been demonstrated and proves to be effective.

Further work is being performed in corroborating this reported correlation with observations at the Barstow-Daggett airport and the AVM at Goldstone. If this proves successful, this may be an effective tool for determining the attenuation statistics near *any* surface observation site following the standards of the Federal Meteorological Handbook.

Acknowledgments

The author would like to thank Nick Konidaris, Abhijit Biswas, Elizabeth Amini, Sabino Piazzola, Gary Spiers, James Lesh, and Nassar Golshan for their consultations and lively discussions.

References

[1] S. Piazzolla, S. Slobin, and P. E. Amini, *Cloud Coverage Diversity Statistics for Optical Communication in the Southwestern United States*, JPL Publication 00-13, Jet Propulsion Laboratory, Pasadena, California, 2000.

[2] B. Sanii, A. Datta, D. Tsiang, J. Wu, and A. Biswas, "Preliminary Results of an Upgraded Atmospheric Visibility Monitoring Station," *The Telecommunications and Mission Operations Progress Report 42-142, April–June 2000*, Jet Propulsion Laboratory, Pasadena, California, pp. 1–12, August 15, 2000. http://tmo.jpl.nasa.gov/tmo/progress_report/42-142/142K.pdf

[3] H. E. Snell, G. P. Anderson, J. Wang, J.-L. Moncet, J. H. Chetwynd, and S. J. English, "Validation of FASE (FASCODE for the Environment) and MODTRAN3: Updates and Comparisons with Clear-Sky Measurements," The European Symposium on Satellite Remote Sensing, Conference on Passive Infrared Remote Sensing of Clouds and the Atmosphere III, Proceedings of the SPIE, Paris, France, 1995.

[4] *Surface Weather Observations and Reports*, Federal Meteorological Handbook (FMH) Number 1, National Weather Service. http://www.nws.noaa.gov/oso/oso1/oso12/fmh1.htm